A Wearable Inertial Sensing Device for Fall Detection and Motion Tracking

Praveen Kumar

Dept. of Biosciences & Bioengineering
IIT Bombay, Mumbai, India
<erpraveen@iitb.ac.in>

Prem C. Pandey

Dept. of Electrical Engineering
IIT Bombay, Mumbai, India
<pcpandey@ee.iitb.ac.in>

***Abstract*— Fall is a major problem for the elderly persons and patients suffering from neuromuscular disorders. A body-worn fall detector can greatly help in providing timely assistance by alerting the emergency services and relatives in case of such an occurrence. A wearable inertial sensing device is developed for fall detection and motion tracking. It consists of an integrated sensor with tri-axial accelerometer and tri-axial gyroscope for sensing linear acceleration and angular velocity, a microcontroller for data acquisition and processing, nonvolatile memory for recording the sensed data, and Bluetooth for wireless connectivity. A fall detection algorithm applying multiple decompositions and thresholding on the acceleration data is implemented for real-time processing using sampling frequency of 100 Hz. The sensed data can be continuously recorded for approximately 10 hours at a sampling frequency of 20 Hz and therefore the device can also be used for actigraphy for diagnosis of sleep disorders. A number of such devices worn on the different parts of the body and wirelessly connected to a central device can be used for continuous tracking of the posture and movement and can serve as an aid for assisted living.**

Keywords*— *assisted living; fall detection; inertial sensing; motion tracking

I. INTRODUCTION

An emerging task of the healthcare system is to provide assisted living to elderly persons and patients suffering from chronic diseases. A patient suffering from neuromuscular disorders has an increased chance of losing balance, which may lead to a fall. A severe fall may cause serious injuries leading to further complications and even death if immediate and appropriate action is not taken. A continuous monitoring of the movement and posture of such individuals would be helpful in alerting the concerned persons for delivering the required assistance and treatment in case of an emergency. Furthermore, a continuous log of movement and posture related data may also be useful for diagnosis and for assessing the effect of the treatment. Persons suffering from sleep disorders are prone to increased risk of heart attack, hypertension, and accidents. A continuous monitoring of posture during sleep can be used as actigraphy data for diagnosis and treatment of sleep disorders.

The motion tracking systems may be based on optical, image, acoustic, magnetic, or inertial sensing. Optical tracking systems detect motion by sensing light patterns, and hence are immune to disturbances due to ferromagnetic and conductive materials in the environment [1], [2]. Image-based systems use multiple cameras for body and face tracking [3], [4] and tend to be relatively expensive. Acoustic sensing systems track motion by determining the velocities and directions of the received acoustic waves [5]. Tilt sensor and magnetometer have also been used to determine the angle of inclination and direction of movement. Inertial tracking systems use low-cost and compact size accelerometers and gyroscopes to sense linear acceleration and angular velocities [6] - [9]. They do not suffer from interference problems and do not impose restrictions on the movement space.

While most of the inertial sensing methods for fall detection are based on accelerometers, some are based on gyroscopes, and some others use multiple sensors. Methods with only accelerometers or with only gyroscopes provide good results for restricted movement in specific directions, while methods using multiple sensors can recognize a larger number of activities with better accuracy [10] - [17]. It is also preferable to have sensors located at different positions of the body to measure the relative movement of various body parts. Head, waist, trunk, and thigh are good locations for sensor placement while wrist is not. For most persons, placing sensors on the head can be uncomfortable. Most signal processing methods for fall detection are difficult to implement on low-power processors in the wearable devices. Methods based on fuzzy inference have been shown to enhance the detection accuracy using a single accelerometer [15], [16] but are not suitable for real-time applications due to their computational complexity. Threshold-based fall detection methods, although having a somewhat lower sensitivity and specificity, are preferable for real-time applications.

A wearable device with inertial sensing and wireless connectivity is developed for fall detection and motion tracking. An integrated sensor with tri-axial accelerometer and tri-axial gyroscope is used for sensing the linear acceleration and angular velocity. Such a sensor helps in reducing the chip count and avoids errors due to mis-alignment of the sensor axes during assembly. A micro-controller is used for signal acquisition, processing, control, and data transfer. The device has nonvolatile memory for recording the sensed data and Bluetooth-based wireless connectivity. A fall detection algorithm, applying multiple decompositions and thresholding on the acceleration data, is implemented on the microcontroller for real-time processing.

The device can also be used as a recording device for actigraphy to assist in the diagnosis of sleep disorders. A number of such small devices worn on the different parts of the body and wirelessly connected to a central device can be used for continuous tracking of the posture and movement of the person and thus can serve as an aid for assisted living.

II. HARDWARE DESIGN

The inertial sensing device is designed for continuously acquiring the acceleration and angular velocity data at a settable sampling frequency of 100 Hz or higher and wirelessly transferring the data to a central device for integration and processing of the data from multiple devices. The device should have on-board processing to detect emergency situations and send an alarm to a base station. To be useful in actigraphy and other motion logging applications, it should have nonvolatile memory to store the acquired data in a time-stamped manner which can be transferred in burst mode. As a body-worn device, it should be light and compact and has to be battery powered with low power consumption. To meet these objectives, the circuit has been designed using a microcontroller and a MEMS-based sensor chip with integrated tri-axial accelerometer and tri-axial gyroscope. Its block diagram is shown in Fig. 1. It has a serially interfaced flash memory for storing the acquired data. For compactness, it is designed without any connectors and switches. A serially interfaced Bluetooth module is provided for wireless data transfer. All components of the circuit are selected to operate at 3.3 V.

A. Component Selection

"InvenSense MPU-6000" [18] is used as the integrated MEMS-based sensor module with tri-axial accelerometer and tri-axial gyroscope. It has on-chip ADC and processor for conversion of the six sensed signals as 16-bit digital outputs, SPI and I2C ports for controlling its operation and transferring the sensed data, and an internal clock for setting the sampling rate and internal processing. The sampling frequency of the on-chip ADC can be selected as 3.9 Hz – 8 kHz. The gyroscope has settable full-scale range of ±250, ±500, ±1000, and ±2000˚/s. The accelerometer has settable full-scale range of ±2, ± 4, ±8, and ±16 *g*. The sensor module has an on-chip digital motion processor for free-fall detection, zero-motion detection, and threshold-based motion detection. At each sampling instant, the 16-bit values of the six channels are stored as 12-byte data. The sensor module has an on-chip 1024-byte FIFO buffer. After the buffer gets filled, an interrupt is generated to enable burst-mode data transfer. The FIFO buffer has a counter associated with it for tracking the number of bytes in the buffer. The chip has a current requirement of 3.9 mA.

The 16-bit microcontroller "Microchip PIC24FJ64GB-004" [19], with 64K program memory and 8K data RAM, 25 I/O pins with programmable functions and two SPI, two I2C, two UART, and one USB for serial I/O, is used as the controller and data processor. The processor starts at power-on with an internal RC oscillator with clock of 8 MHz, which can be divided by 2 – 256 to obtain a lower clock. The internal instruction cycle clock is half of the processor clock.

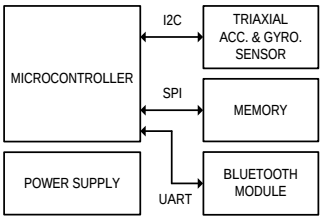

Fig. 1. Block diagram of the inertial sensing device.

The sampling frequency of the sensor module is derived from its own on-chip clock and is thus not affected by the accuracy of the microcontroller clock. With processor clock of 8 MHz, its current requirement is 2.9 mA.

"Microchip SST25VF064C" [20] has been used as a 64M bit serial I/O flash memory. At each sampling instant, the 6 sensor outputs (tri-axial accelerometer and tri-axial gyroscope) give 12 bytes of data. Thus the memory has a storage capacity of 699,050 samples (8M bytes / 12 bytes). At a sampling frequency of 100 Hz (as generally used for fall detection and motion tracking), the memory can record data for approximately 2 hours. For actigraphy and applications involving recording at a lower sampling frequency of 20 Hz, the memory can store data for approximately 10 hours. It has SPI and 256-byte buffer for serial I/O. The data are written into the input buffer and are saved by sending the starting address and a page-write instruction, which takes about 2.5 ms. For sample-by-sample signal acquisition at a sampling frequency of 100 Hz, the six sensor channels result in 12 bytes every 10 ms. These are appended with two bytes as time index and written to the input buffer. With the instruction cycle clock of 4 MHz, transferring 14 bytes to the buffer and giving the page-write instruction take about 1.64 ms. Thus the memory write speed is adequate for storing the sensed data even on sample-by-sample basis. The current requirement of the chip is 12 mA during read operation, 25 mA during write/erase operation, and 5 µA in standby mode.

For short-range wireless data transfer, the Bluetooth module "Roving Network RN-42" [21] has been used. It has a range of 20 m and supports UART data rate up to 240 kbps in slave mode and 300 kbps in master mode. The rate of data transfer with the microcontroller is settable as 1.2 – 921 kbps. Its current requirement is 26 µA in sleep mode, 3 mA when connected, and 30 mA during wireless data transfer. The sum of the current requirements of all circuit components is 62 mA (microcontroller: 2.9 mA, sensor: 3.9 mA, memory: 25 mA, Bluetooth module: 30 mA). As the memory read-write and wireless data transmission do not take place simultaneously, the maximum current requirement of the circuit is estimated to be 36 mA, , The circuit is powered using 3.3 V linear regulator "Microchip MCP 1802" [22] with 200 mV dropout and 300 mA output current.

B. Interconnections and Circuit Assembly

The connections to the microcontroller U5 are shown in Fig. 2. As the analog blocks of the microcontroller are not used, the pins AVDD and AVSS are shorted to the pins DVDD and DVSS, respectively. The connector CN1 is provided for inline programming and debugging. The sensor

U4 is interfaced to the microcontroller using I2C, as shown in Fig. 3. It needs two lines (SCK, SDA) and has a built-in acknowledgment and addressing. Its data rate is sufficient for transferring the data for sampling rate of up to 1 kHz.

The Bluetooth module U3 is interfaced with micro-controller U5 using UART as shown in Fig. 4. The pins Rx and Tx of U3 and the pins RP19 and RP20 of the microcontroller are connected to the 5-pin connector CN2 for debugging. The jumpers J1 and J2 short RP19 to Rx and RP20 to Tx, respectively. The baud rate setting pin PIO7 is not connected and therefore the baud rate gets set as 115 kbps at power-on. There are two LEDs (red and green) to indicate the operation status of the module. The red one blinks at the rate of 2/s at boot up, 10/s during configuration, and 1/s when the module is idle and discoverable. It is continuously lit when the connection is established. The green one blinks during data transfer. The address, name, baud rate, parity, mode (master, slave), pin code, remote address, etc. are set in the configuration mode, which is entered by sending '$$$'. The other operations are controlled by specific I/O pins: PIO6 to set the module in master mode, PIO4 to set factory defaults, PIO3 to enter auto discovery mode, and PIO2 to convey the connection status to the microcontroller. The flash memory U1 is interfaced to the microcontroller U5 using SPI (pins SO, SI, SCK, CE) as shown in Fig. 5. The pin WP is for hardware control of write protection. The pin HOLD is for pause in a serial sequence and power-on reset.

A 2-layer PCB (36.32 mm x 29.21 mm) was designed for the circuit with both sides of the board used for placing SMD components in order to reduce its area. The assembled PCB, the Bluetooth module, and the battery were housed in an acrylic box [23].

III. Data Acquisition and Testing

The device has no switches and connectors and the control and data transfer are handled through the Bluetooth module. The microcontroller program has a main part for initialization and a set of interrupt service routines (ISR) for carrying out specific operations in response to UART interrupt from the Bluetooth module. After power-on, the main program sets the RC oscillator clock of 8 MHz as the processor clock, resulting in the instruction cycle clock at 4 MHz. The microcontroller I/O port pins are initialized in accordance with the functions as shown in Fig. 2 – Fig. 5. The UART-1, SPI-1 and I2C-2 modules are enabled. The UART-1 baud rate is set to 115 kbps and the receive interrupt is enabled with highest priority. The SPI-1 clock is same as the internal instruction cycle clock, while the I2C-2 clock is set at 100 kHz. The sensor is reset. The full-scale ranges of accelerometer and gyroscope are set to ±4 *g* and ±500 °/s, respectively. Its FIFO is enabled and the digital motion processor and internal high-pass and low-pass filters are disabled. The sampling frequency of both accelerometer and gyroscope is set as 100 Hz. The BPL (block protection lock) bit is set to allow hardware control over the write protection of the status register using the WP pin. The microcontroller is placed in sleep mode to save power. It comes out of this mode on receiving a sensor interrupt or

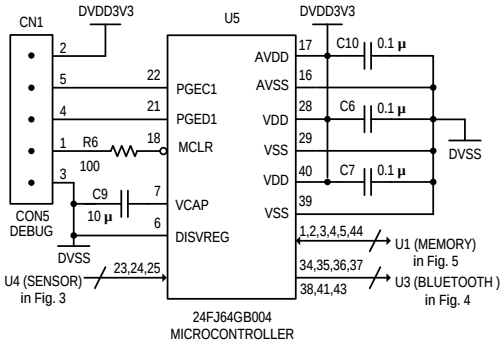

Fig. 2. The microcontroller pin connections.

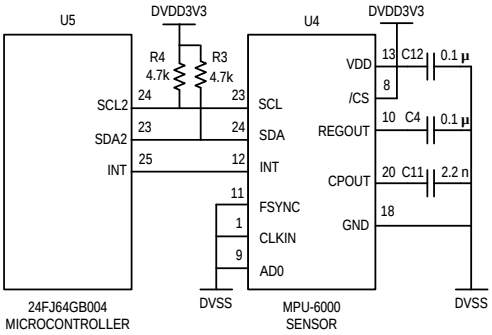

Fig. 3. Sensor interfacing.

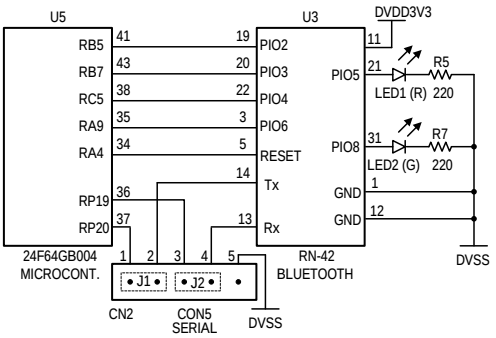

Fig. 4. Serial communication and Bluetooth wireless interface.

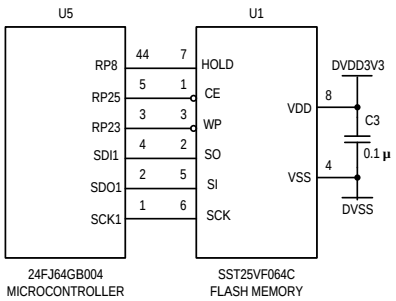

Fig. 5. Memory interfacing.

UART interrupt to execute the respective ISR. Single character codes are assigned for commands from the Bluetooth module: 'p' to start data acquisition, 's' to stop data acquisition, 'r' to retrieve stored data, 'n' to retrieve last *N* bytes, and 'e' to erase the flash memory. The motion tracking data can be acquired from the device using "sample-by-sample mode" or "burst mode".

A. Data Acquisition

This mode is used for sample-by-sample transfer of data from the sensor to the microcontroller. For page-write to the flash memory, a 252-byte (21 samples x 12 bytes/sample) data buffer in the microcontroller data RAM, a buffer pointer, and a memory page pointer are used. After receiving 'p' in the UART-Rx register, the sensor interrupt is enabled and set to "data ready enable" mode. The microcontroller is placed back in sleep mode. After the sensor is ready with the six-channel data, a sensor interrupt is raised and the sensor ISR is executed. The 12-byte data are read from the sensor and stored in the data buffer, the buffer pointer is incremented by 12, and the external interrupt flag is cleared. The microcontroller is placed in sleep mode if the buffer is not full. If the buffer is full, the contents are transferred to the flash memory buffer and stored using page write instruction. The memory page pointer is incremented, the buffer pointer is reset, the interrupt flag is cleared, and the microcontroller is placed in sleep mode until another interrupt is raised. This sample-by-sample acquisition is continued until 's' is received in the UART-Rx register. For 100 Hz sampling frequency, an interrupt is generated every 10 ms and therefore not much time is available for signal processing.

The sensor has FIFO buffer of 1024 bytes (85 samples and 4 bytes). With sampling frequency of 100 Hz, the buffer gets filled after 860 ms, and therefore use of burst mode of data transfer significantly reduces the overheads related to saving the data into the flash memory and significantly increases the time available for block-mode signal processing. As the buffer size is not an integer multiple of 6-axis data size (12 bytes), use of sensor interrupt for data transfer results in loss of one sample in every read cycle. Therefore the transfer is handled by polling the FIFO counter register. In this mode, the sensor interrupt is not enabled; and the FIFO counter register is read to find out if N bytes have been acquired. The bytes are read into a buffer in the microcontroller data RAM, and then written into the flash memory using page-write instruction. Meanwhile if data retrieve request is received in the form of 'n' in the UART-Rx register, the bytes are output through UART-Tx register to the Bluetooth module. The data acquisition loop is stopped if 's' is received in UART-Rx register. The value of N should be selected such that the time corresponding to N/12 samples is more than the time needed for storing and processing the data block, and that the delay of N/12 samples in fall detection is acceptable. With N = 252, the block has 21 samples and its duration is 210 ms for 100 Hz sampling. These data bytes are stored using a single page-write instruction, leaving most of the time for signal processing.

B. Testing and Calibration

A graphical user interface (GUI) was developed to control the device operations through a PC with Bluetooth connectivity. The program can be used for data acquisition by the device and for transferring the previously acquired data to PC. The sensor data are in 2's complement format and are transmitted by the device in hexadecimal format. The data are saved on PC as a text file with each row starting with the sample number followed by three-axis data of the accelerometer and three-axis data of the gyroscope (time, accl_x, accl_y, accl_z, gyro_x, gyro_y, and gyro_z). The accelerometer data are converted into gravitational unit (g) and the gyroscope data are converted into angular rate data (°/s) and these are displayed on the GUI screen and stored for further processing [23].

The device operation was tested by using a test setup with the Control Moment Gyroscope (CMG) "Model 750" [24], with a central platform with two outer rings allowing freedom of three degrees of rotation, as shown in Fig. 6. It has an encoder at each axis to record the angle of rotation and the instrument is connected to a PC for recording the angular locations with respect to time. The initial position of the platform and the outer rings can be fixed by applying the brakes provided for each axis. The sensed angular positions can be differentiated to get the corresponding angular velocities. The inertial sensing device was fixed on the platform. For testing of the static operation, the brakes were applied on two axes such that the angle between them was 90°. The device orientation was fixed at angles of 0°, 30°, 45°, 60°, and 90° about the third axis. The sensor data were recorded for each angle in sample-by-sample mode at a sampling frequency of 100 Hz for 10 s. This process was repeated for all the three axes. The mean and standard deviation of the samples for each angle around each axis was calculated. The gyroscope readings had a mean value of nearly 0 °/s for each axis in all orientations, and the maximum standard deviation was 0.1451 °/s, indicating that the offset and drifts were not significant. The accelerometer outputs closely matched the expected values. The maximum deviations in the X, Y, and Z axis values of the accelerometer were 0.0627 g, 0.0098 g, and 0.0861 g, respectively.

For testing the gyroscope, the device was subjected to an oscillatory motion about each of the three axes by to-and-fro movement of the platform or the outer rings. The start buttons of the two data acquisition programs were pressed simultaneously and the data were collected at a sampling frequency of 100 Hz. The angular location data from CMG were converted to angular velocity data by differentiating it (using Matlab function "diff"). The plots of the angular velocities sensed by the inertial sensing device closely matched the corresponding plots obtained from the encoder data. An example of these plots is given in Fig. 7.

IV. Real-time Fall Detection

A fall detection algorithm suitable for real-time processing using the microcontroller of the inertial sensing device has been developed. As fusion of the accelerometer and gyroscope data is computation intensive, the proposed algorithm is based on application of multiple decompositions and thresholding on the acceleration data. Let us represent the acceleration components along the three axes as A_x, A_y, A_z, respectively. As the axial outputs get affected by changes in the orientation of the sensor, it is proposed to monitor changes in magnitude of the acceleration along multiple directions. For this purpose, we used seven variables: A_x, A_y,

A_z, $A_{xy} = \sqrt{(A_x^2+A_y^2)}$, $A_{yz} = \sqrt{(A_y^2+A_z^2)}$, $A_{zx} = \sqrt{(A_z^2+A_x^2)}$, and $A_{xyz} = \sqrt{(A_x^2+A_y^2+A_z^2)}$.

A. Exploratory Experiment

As an exploratory experiment, recordings were made during simulated movements of the sensing device worn at the waist. The device was attached to a waist-high wooden pole near its top end and the pole was positioned vertically, with the y-axis of the sensor aligned in the vertical direction, the z-axis in the forward horizontal direction, and the x-axis in the sideways horizontal direction. The pole was made to fall in several directions and the data were acquired using burst mode of data transfer. The seven parameters were plotted with respect to time, as shown in Fig. 8. The initial value of A_y is 1 g as it is initially parallel to the gravitational axis, while the initial values of A_x and A_z are zero. The initial value of A_{zx} is zero and the initial values of all other variables are 1 g. There is a sudden dip in the value of A_y as the device undergoes a free fall under the influence of the gravity. This dip is reflected in all other plots except A_{zx}. After the dip, the impact of the fall results is an oscillation in all components: with maximum amplitude and duration in A_z for forward and backward falls and in A_x for left and right falls. These oscillations contribute to large positive peaks in A_{xy}, A_{yz}, A_{zx}, and A_{xyz} plots. All kind of simulated falls show large oscillations in at least some of the variables. Swinging and other motions of the pole do not show such oscillations.

B. Fall Detection Algorithm

The proposed method for fall detection is based on monitoring the magnitudes of three axial components of the acceleration, magnitudes in three orthogonal planes, and the total magnitude. The fall detection is based on the observation that a fall is associated with a large change from the mean value in at least one of these seven variables and that the change lasts for a certain minimum duration and it does not exist for too long a duration. A change extending over a long duration is likely to be associated with an activity of daily life and not with a fall.

At each sampling instant, we calculate seven variables from the three acceleration components as the following:

$$v_1(n) = \left| A_x(n) \right|$$
$$v_2(n) = \left| A_y(n) \right|$$
$$v_3(n) = \left| A_z(n) \right|$$
$$v_4(n) = \sqrt{[(A_x(n))^2+(A_y(n))^2]}$$
$$v_5(n) = \sqrt{[(A_y(n))^2+(A_z(n))^2]}$$
$$v_6(n) = \sqrt{[(A_x(n))^2+(A_z(n))^2]}$$
$$v_7(n)=\sqrt{[(A_x(n))^2+(A_y(n))^2+(A_z(n))^2]}$$

For each of these variables, a 100-point moving average is calculated as

$$m_i(n) = m_i(n-1) + [v_i(n) - v_i(n-100)]/100 \quad (1)$$

With a sampling rate of 100 Hz, this corresponds to moving average over 1 s duration. Change in the variable from the moving average is calculated as

$$d_i(n) = |v_i(n) - m_i(n)| \quad (2)$$

Fig. 6. Control Moment Gyroscope Model 750 [24].

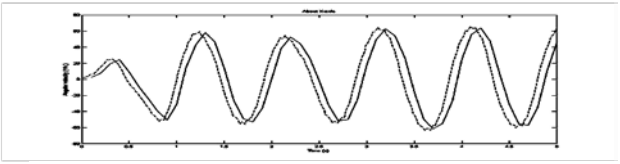

Fig. 7. X-axis gyroscope outputs (solid: sensor, dotted: CMG).

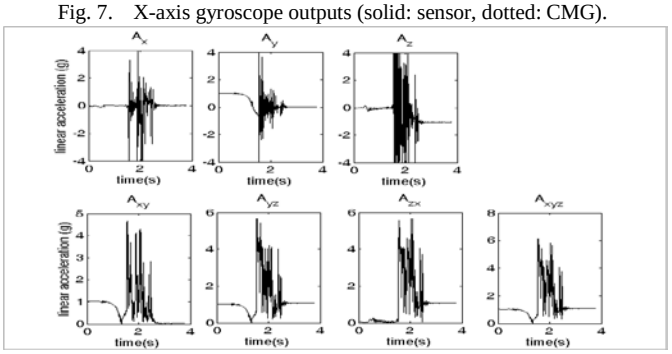

Fig. 8. Fall forward: Accelerometer outputs and calculated magnitudes.

Each d_i is compared with a threshold θ, and if the value remains supra-threshold for a duration greater than t_1 but not greater than t_2, it is considered to be indicating a fall. The duration thresholds $t_1$and t_2 are the minimum and maximum estimates of the duration for which a fall can last. If d_i becomes less than the threshold θ before the duration t_1, the variable duration is reset and the algorithm starts afresh. If d_i remains greater than θ for longer than t_1, it is checked for becoming smaller than θ and if it becomes smaller earlier than t_2, it is inferred that the variable has indicated a fall and the detection process starts afresh. If d_i remains greater than θ for longer than t_2, it is inferred that the variable is indicating an oscillatory change due to activities of daily life and hence is ignored until it becomes less than θ, after which the detection process starts afresh. The detection process is simultaneously applied on all seven variables. The fall is declared if it is detected for at least one of the variables.

C. Test Results

Fall detection was tested for various types of simulated falls with the device attached to a pole as in case of exploratory experiment, with each fall type repeated 5 times. All falls were detected correctly. For activities of daily life, the device was worn by a person on the waist. The fall detection algorithm was able to discriminate the activities of daily life from simulated falls by choosing θ = 2g, t_1 = 250 ms, and t_2 = 850 ms. Over an extended use, there was no fall detection during activities of daily life and there was no missed fall detection during simulated falls. Thus the results indicated 100% sensitivity and specificity. A detailed

examination of the results showed that d_i' along the gravitational axis, in the three orthogonal planes, and the total magnitude always detected the fall. During the activities of skipping, jogging, and fast sitting, some of the d_i's crossed θ but for duration less than t_1 and hence these activities were not detected as fall. During other activities, the thresholds were never crossed. The results show that the algorithm detects the falls with any orientation of the device.

V. CONCLUSIONS

A wearable inertial sensing device for continuously sensing and recording the motion related variables, transmitting the data wirelessly, and alerting a base station on detecting a fall has been developed. The design uses an integrated MEMS-based sensor with tri-axial accelerometer and gyroscope along with a microcontroller. The data may be recorded for approximately 2 hours at a sampling frequency of 100 Hz. A Bluetooth module provides wireless connectivity for data transfer without using any switches and connectors. The circuit operates at 3.3 V with a current of less than 40 mA during its operation and 3 mA during sleep mode. The data from multiple devices can be transferred to a central device in a time multiplexed manner. A real-time algorithm for fall detection using the acceleration data has been developed and tested. It applies thresholding on the change from the moving average on multiple decompositions of the acceleration. It results in separation of activities of daily life from the fall and the fall detection works with any orientation of the waist-worn device. As part of future work, the device needs to be extensively tested, particularly under realistic fall conditions on a large number of human subjects. These tests will be useful in selecting the most appropriate values of the processing parameters. Fusion of accelerometer and gyroscope data and fusion of data from multiple devices can help in further extending the application of the device as an aid for assisted living.

ACKNOWLEDGMENT

The authors are grateful to Prof Hemendra Arya and Mr Sourav Chatterjee for use of the CMG test facility in the Dynamics and Control Lab of the Department of Aerospace Engineering, IIT Bombay and to Dr Niranjan Khambete for inputs on the paper.

REFERENCES

[1] G. Welch, G. Bishop, L. Vicci, S. Brumback, K. Keller, and D. Coluccit, "The HiBall tracker: high-performance wide-area tracking for virtual and augmented environments," in Proc. ACM Symp. Virtual Reality Softw. Technol., London, Dec. 1999, pp. 1-11.

[2] W. Korb, D. Engel, R. Boesecke, G. Eggers, B. Kotrikova, R. Marmulla, J. Raczkowsky, H. Worn, J. Muhling, and S. Hassfeld Development and first patient trial of a surgical robot for complex trajectory milling. Comput. Aided Surg., vol. 8(5), pp.247-256, 2003.

[3] T. Lee and A. Mihailidis, "An intelligent emergency response system: preliminary development and testing of automated fall detection," Telemed. and Telecare, vol. 11, pp. 194-198, 2005.

[4] Vicon, "Case study: The dance of love", Available: http://www.vicon.com/company/documents/Northumbria_owres.pdf

[5] O. Gabai and H. Primo, "Acoustic motion capture," US Patent Application 20110009194, 2011.

[6] X. Yun and R. Bachmann, "Design, implementation, and experimental results of a quaternion-based Kalman filter for human body motion tracking," IEEE Trans. Robotics., vol. 22(6), pp. 1216–1227, Dec. 2006.

[7] A. Gallagher, Y. Matsuoka, and W. T. Ang, "An efficient real-time human posture tracking algorithm using low-cost inertial and magnetic sensors," in Proc. IEEE Int. Conf. Robot. Autom., Sendai, Japan, Sep. 28–Oct. 2, 2004, pp. 2967-2972.

[8] J. S. Wang, Y. L. Hsu, and J. N. Liu, "An inertial measurement unit based pen with a trajectory reconstruction algorithm and its applications," IEEE Trans. Ind. Electron., vol. 57(10), pp. 3508-3521, 2010.

[9] R. Zhu and Z. Zhou, "A real-time articulated human motion tracking using tri-axis inertial/magnetic sensors package," IEEE Trans. Neural Syst. Rehab. Eng., vol. 12(2), pp. 295-302, 2004.

[10] M. Kangas, A. Konttila, I. Winblad, and T. Jamsa, "Determination of simple thresholds for accelerometry-based parameters for fall detection," in Proc. 28th IEEE Int. Conf. Engineering in Medicine and Biology Society, Lyon, France, 13-28 Aug. 2007, pp. 1367-1370.

[11] A. K. Bourke, J. V. O'brien, and G. M. Lyons, "Evaluation of a threshold-based tri-axial accelerometer fall detection algorithm," Gait & Posture, vol. 26(2), pp. 194-199, 2007.

[12] A. K. Bourke, and G. M. Lyons, "A threshold-based fall-detection algorithm using a bi-axial gyroscope sensor," Medical Engg. Physics, vol. 30(1), pp. 84-90, 2008.

[13] J. Y. Hwang, J. M. Kang, Y. W. Jang, and H. C. Kim, "Development of novel algorithm and real-time monitoring ambulatory system using Bluetooth module for fall detection in the elderly," in Proc. 26th IEEE Int. Conf. Engineering in Medicine and Biology Society, San Francisco, CA, 2004, vol.1, pp. 2204-2207.

[14] Q. Li, J. A. Stankovic, M. A. Hanson, A. T. Barth, J.Lach, and G. Zhou, "Accurate, fast fall detection using gyroscopes and accelerometer-derived posture information," in Proc. 6th Int. Workshop on Wearable and Implantable Body Sensor Networks, Berkeley, CA, 2009,pp. 138-143.

[15] M. Helmi and S. M. T. Almodarresi, "Human activity recognition using a fuzzy inference system," in Proc. 18th IEEE Inter. Conf. Fuzzy System, Jeju island, Korea, 2009, pp.1897-1902.

[16] J. Y. Yang, Y. P. Chen, G. Y. Lee, S. N. Liou, and J. S. Wang, "Activity recognition using one tri-axial accelerometer: a neuro-fuzzy classifier with feature reduction," in Proc. Int. Conf. Entertainment Computing, Shanghai, 2007, vol. 4740, pp. 395-400.

[17] C. Dinh, D. Tantinger, and M. Struck, "Automatic emergency detection using commercial accelerometers and knowledge-based methods," Comput. Cardiology, vol. 36, pp. 485-488, 2009.

[18] InvenSense, "Motion processing unit product specification rev. 3.2, MPU-6000", 16th Nov, 2011. [online]. Available: http://www.invensense.com/mems/gyro/documents/PS-MPU-6000A.pdf

[19] Microchip Technology, "PIC24FJ64GB004 family data sheet", 15th July, 2010. [online]. Available: http://www.microchip.com/downloads / en/DeviceDoc/39940d.pdf

[20] Microchip Technology, "64-Mbit SPI serial dual I/O flash, SST25VF064C", 11th June, 2011. [online]. Available: http://www.microchip.com/downloads/en/DeviceDoc/25036A. pdf

[21] Roving Networks, "Class 2 Bluetooth module version 1.08, RN-42", 11th Aug, 2010. [online]. Available: http://www.rovingnetworks.com/resources/download/19/RN_42.pdf

[22] Microchip Technology, "MCP 1802", 8th Dec, 2006. [online]. Available: http://www. microchip.com/downloads/en/DeviceDoc/22053C.pdf

[23] P. Kumar, "An inertial sensing module for movement and posture monitoring for assisted living," M. Tech. dissertation, Biomedical Engineering, Indian Institute of Technology Bombay, 2013.

[24] Educational Control Products, "Model 750 Control Moment Gyroscope", 12th June, 2012. [online]. Available: http://www.ecpsystems.com/docs/ECP_Gyroscope_Model_750.pdf